J Pharmacol Sci **91**, 23 – 33 (2003)

Journal of Pharmacological Sciences

Full Paper

Integrity of Actin-Network Is Involved in Uridine 5'-Triphosphate Evoked Store-Operated Ca^{2+} Entry in Bovine Adrenocortical Fasciculata Cells

Masahiro Kawamura[1,*], Osamu Terasaka[2], Takanori Ebisawa[1], Ichiro Kondo[1], Eiji Masaki[1], Ashram Ahmed[3] and Miyuki Kagata[1]

[1]*Department of Pharmacology (I), Jikei University School of Medicine, 3-25-8 Nishi-Shinbashi, Minato-ku, Tokyo 105-8461, Japan*
[2]*Division of Biology, Jikei University School of Medicine, 8-3-1 Kokuryo, Chofu-shi, Tokyo 182-8570, Japan*
[3]*Department of Anesthesiology, Ain Shams University, Cairo, Egypt*

Received May 20, 2002; Accepted October 9, 2002

Abstract. Store-operated Ca^{2+} entry channels (SOCs) play an important role in the regulation of diverse non-excitable cell functions. However, the precise mechanism of SOCs activation is still controversial. Uridine 5'-triphosphate (UTP) was shown to induce Ca^{2+} entry in a dihydropyridines-insensitive manner and accelerated steroidogenesis in bovine adrenocortical fasciculata cells (BAFCs) via the Gq/11 protein-coupled $P2Y_2$ receptor. Therefore we investigated whether UTP is involved in SOCs activation and the mechanism of UTP-induced SOCs activation. Fura 2-loaded BAFCs were used for the measurement of intracellular concentration of Ca^{2+} ($[Ca^{2+}]_i$) mobilization. Extracellular UTP evoked Ca^{2+} release from intracellular stores followed by an increase in Ca^{2+} entry. The Ca^{2+} influx elicited by UTP was inhibited not by nifedipine, but by Zn^{2+}, Cd^{2+}, and Ni^{2+} (potency order: $Zn^{2+} > Cd^{2+} \gg Ni^{2+}$), and the effect of UTP was also attenuated by a phospholipase C inhibitor (U73122). These results indicate that UTP activates SOCs in BAFCs. The increase in $[Ca^{2+}]_i$ by UTP was attenuated by ML-9, a myosin-light chain kinase inhibitor, and calmodulin inhibitors, W-7 and E6 berbamine, in a concentration-dependent manner. These reagents depolymerized actin filaments with rhodamine staining in BAFCs. Cytochalasin D also inhibited UTP-activated SOCs and depolymerized actin filaments. From these results, we proposed that calcium/calmodulin dependent myosin-light chain kinase is involved in the mobilization of actin filaments and the integrity of actin-network plays an important role in UTP-induced SOCs activation in BAFCs.

Keywords: cytoskeleton, actin-filament, UTP, store-operated Ca^{2+} entry, adrenal

Introduction

$[Ca^{2+}]_i$ mobilization plays an important role in the regulation of fundamental cell functions. There are three Ca^{2+} influx pathways in vertebrate cells, VOCs, ligand-gated non-specific cation channels, and ROCs. One of the ROCs is thought to be the SOCs (1). When Gq/11 protein-coupled receptors are occupied by pertinent

*Corresponding author. FAX: +81-3-5473-1428
E-mail: pharmacology@jikei.ac.jp

Abbreviations used are (in alphabetical order): ATP, adenosine 5'-triphosphate; BAFC, bovine adrenocortical fasciculata cell; BSA, bovine serum albumin; $[Ca^{2+}]_i$, intracellular concentration of Ca^{2+}; Ca^{2+}/CaM kinase II, Ca^{2+}/calmodulin-dependent protein kinase II; CPA, cyclopiazonic acid; ER, endoplasmic reticulum; F-actin, actin filaments; fura 2/AM, fura 2/acetoxymethylester; I_{CRAC}, calcium release-activated calcium current; $InsP_3$, inositol 1,4,5-trisphosphate; KN-62, 1-[*N,O*-bis(5-isoquionolinesulfonyl)-*N*-methyl-L-tyrosyl]-4-phenylpiperazine; ML-9, 1-(5-chloronaphthalene-1-sulfonyl)-1*H*-hexahydro-1,4-diazepine; MLCK, myosin-light chain kinase; PBS, phosphate-buffered saline; ROC, receptor-operated Ca^{2+} channel; SOC, store-operated Ca^{2+} channel; TG, thapsigargin; TRP, transient receptor potential; U73122, 1-[6(17β-3-methoxyestra-1,3,5(10)-trien 17-yl)amino)hexyl]-1*H*-pyrrole-2,5-dione; UTP, uridine 5'-triphosphate; VOC, voltage-operated Ca^{2+} channel; W-7, *N*-(6-aminohexyl)-5-chloro-1-naphthalenesulfonamide; W-5, *N*-(6-aminohexyl)-1-naphthalenesulfonamide.

ligands in non-excitable cells, phospholipase Cβ is activated to accelerate $InsP_3$ biosynthesis. $InsP_3$ acts on its receptors in ER followed by release of the luminal Ca^{2+} into the cytosol. The Ca^{2+} store depletion triggers Ca^{2+} influx from an extracellular pool via SOCs (2). Although several hypotheses were proposed, the precise mechanism of SOCs activation is still uncertain (3).

Recently, extracellular ATP and UTP are regarded as physiological ligands in diverse cells and tissues via nucleotide receptors (4, 5). Nucleotide receptors are classified into two types, a ligand-gated P2X and a G protein-coupled P2Y (5). Kawamura et al. (6, 7) and Hoey et al. (8) reported that P2Y receptors were involved in steroidogenesis in BAFCs. Both ATP and UTP enhanced steroidogenesis through Ca^{2+} influx from an extracellular pool via the $P2Y_2$ receptor in BAFCs (9).

UTP is a potent physiological agonist on Gq/11 protein-coupled $P2Y_2$ receptors (10). In BAFCs, UTP enhances intracellular $InsP_3$ followed by Ca^{2+} release from ER and induces Ca^{2+} influx from the extracellular pool (9). Also, the presence of SOCs in BAFCs has been reported by Kondo (11). These observations suggest that UTP might activate SOCs in BAFCs.

From recent knowledge about the physiological role of cytoskeletons in the regulation of cellular function, it has been elucidated that the filamentous network of F-actin, intermediate tubules, and microtubules plays a pivotal role in diverse cell signalings (12). In $[Ca^{2+}]_i$ mobilization, it has been reported that a MLCK inhibitor attenuates carbachol-activated nonselective cationic current in guinea pig gastric myocytes (13) and also inhibits SOCs in endothelial cells (14, 15). Although they suggested the contribution of F-actin on SOCs activation, morphological change in the cells by the agent had not been proposed. In the present paper, we investigated the effect of MLCK inhibitor on UTP-induced SOCs activation and the actin-network in BAFCs.

Materials and Methods

Primary culture of BAFCs

Bovine adrenocortical cells were isolated aseptically using collagenase and deoxyribonuclease I as previously described (16). The isolated cells were cultured in Ham's F-10 medium supplemented with 5% fetal calf serum, 10% newborn calf serum, 2.5% horse serum, and antibiotics on a coverslip coated with collagen (16, 17). Three-day primary cultured monolayer cells were used for the experiments.

Measurement of $[Ca^{2+}]_i$

$[Ca^{2+}]_i$ was monitored as described by Ebisawa et al. (17). Briefly, BAFCs on a coverslip were loaded with 5 μM fura 2/AM in Krebs-Ringer HEPES buffer (123.4 mM NaCl, 6 mM KCl, 1.2 mM KH_2PO_4, 1.2 mM $MgSO_4$, 1.2 mM $CaCl_2$, 2 mg/ml glucose, 2 mg/ml BSA, 10 mM HEPES, pH 7.4) supplemented with 0.02% cremophor EL for 90 min at 37°C. The fura 2-loaded cells were incubated in the above buffer without cremophor EL in a quartz cell with continuous stirring at 30°C. In the experiments in which Zn^{2+}, Cd^{2+}, and Ni^{2+} were used, a HEPES buffer (127 mM NaCl, 6 mM KCl, 1.2 mM $MgSO_4$, 1.2 mM $CaCl_2$, 2 mg/ml glucose, 2 mg/ml BSA, 10 mM HEPES, pH 7.4) was applied to avoid the precipitation of these cations. The fluorescence intensity was monitored by spectrofluorometer at an emission wavelength of 510 nm, while the excitation wavelength between 340 and 380 nm. The increase in $[Ca^{2+}]_i$ was expressed as the ratio of the fluorescence intensity excited at 340 nm to that of 380 nm (I_{340}/I_{380}). The Ca^{2+}-imaging in a sigle cell was studied by use of Aqua Cosmos (Hamamatsu Photonics, Hamamatsu).

Fluorescent staining of F-actin

Fluorescent staining of F-actin was performed by the modification of the method of Tang et al. (18). In brief, BAFCs cultured on a coverslip were rinsed in PBS for 5 min and fixed in 10% formaldehyde in PBS for 5 min at room temperature. After the cells were rinsed again in PBS for 5 min, they were rendered permeable with 0.1% Triton X-100 in PBS for 5 min and incubated with rhodamine-phalloidin, diluted 1:10 with PBS, for 20 min at 37°C. The fluorescence image was viewed on Nikon Microphoto-FX microscope (Nikon Industry, Tokyo) and photographed on Kodak Tri-X pan film. Cell morphology was visualized by a phase-contrast microscopy.

Statistics

The statistical analysis was carried out using analysis of variance and Student's *t*-test. The value of $P<0.05$ was considered to be statistically significant.

Materials

The materials were purchased from the following companies: UTP (Yamasa Co., Chiba); U73122 and ML-9 (Wako Pure Chemical Industries, Ltd., Osaka); fura 2/AM (Dojindo Lab., Kumamoto); collagenase (Funakoshi Co., Tokyo); W-7 and W-5 (Seikagaku Co., Tokyo); deoxyribonuclease I, nifedipine, CPA, TG, and KN-62 (Sigma Chemical Co., St. Louis, MO, USA); E6 berbamine (Biomol Research Laboratories Inc., Plymouth, PA, USA); Ham's F-10 medium (Gibco Laboratories, Inc., New York, NY, USA); rhodamine-phalloidin (Molecular Probes, Inc., Eugene, OR, USA).

All the other chemicals were of reagent grade.

Results

Effect of U73122 on UTP-induced $[Ca^{2+}]_i$ mobilization

As shown in Fig. 1, extracellular UTP (10 μM) increased $[Ca^{2+}]_i$ in a biphasic manner in the presence of extracellular Ca^{2+} (1.2 mM) in BAFCs. The first phase was fast and transient, and the second one was sustained. When the extracellular Ca^{2+} was abolished by the addition of 2 mM EGTA, only the first phase was observed. The results indicate that the first phase is induced by Ca^{2+} release from intracellular stores, and the second phase is formed by Ca^{2+} influx from an extracellular pool in BAFCs. UTP increased both phases concentration-dependently, and 10 μM UTP showed the maximum effect (data not shown). Thus 10 μM UTP was used in the following experiments. The addition of 10 μM nifedipine, a VOC inhibitor, did not attenuate the second phase (Fig. 1A). Therefore VOCs should not be involved in the Ca^{2+} influx pathway activated by UTP. U73122, a phospholipase C inhibitor (19), inhibited the increase in $[Ca^{2+}]_i$ induced by 10 μM UTP in a concentration-dependent manner (5 – 10 μM) (Fig. 1B). The inhibitor attenuated both the first and the second phases. U73122 at 10 μM inhibited both phases significantly. However, 10 μM U73343, an inactive U73122 derivative, showed only a weak inhibitory effect on 10 μM UTP-induced $[Ca^{2+}]_i$ mobilization in BAFCs (data not shown).

Effects of Zn^{2+}, Cd^{2+}, and Ni^{2+} on UTP-induced $[Ca^{2+}]_i$ mobilization

We examined the effects of Zn^{2+}, Cd^{2+}, and Ni^{2+}, calcium release-activated calcium current (I_{CRAC}) inhibitors (20), on the UTP-induced $[Ca^{2+}]_i$ mobilization in BAFCs. The pretreatment of Zn^{2+}, Cd^{2+}, and Ni^{2+} also attenuated the second phase of UTP-induced increase in $[Ca^{2+}]_i$. The ratio at 200 s from the beginning of fluorescence determination is shown in Fig. 2. The potency order is $Zn^{2+} > Cd^{2+} \gg Ni^{2+}$.

Effect of ML-9 on UTP-induced $[Ca^{2+}]_i$ mobilization

The effect of ML-9, a MLCK inhibitor (21), on 10 μM UTP-induced $[Ca^{2+}]_i$ mobilization in fura 2-loaded BAFCs in the presence of extracellular Ca^{2+} (1.2 mM) was examined. Pretreatment with ML-9 (25 and 50 μM) for 10 min attenuated the second phase evoked by UTP. However, the first phase was not affected by ML-9 (Fig. 3A). The inhibitory effect of 25 and 50 μM ML-9 on the second phase was statistically different from control value (P<0.05) (Fig. 3B).

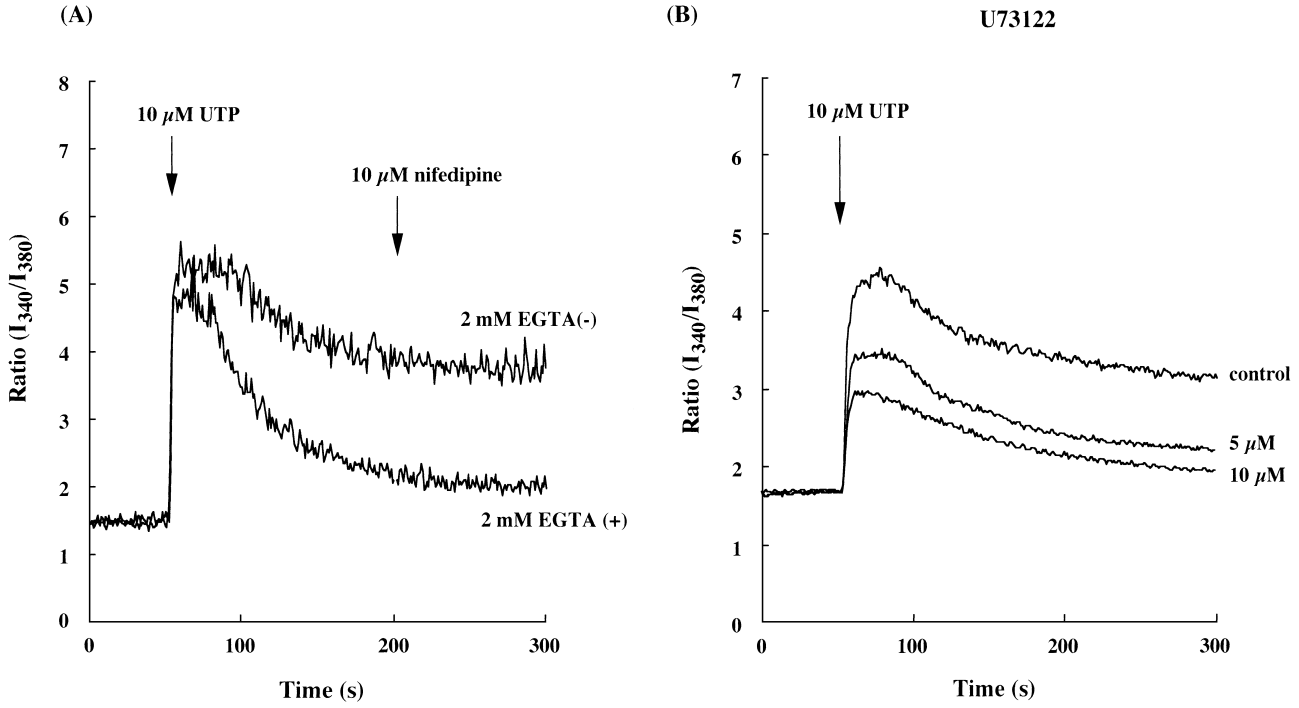

Fig. 1. $[Ca^{2+}]_i$ mobilization by UTP in BAFCs. A: Effects of UTP on $[Ca^{2+}]_i$ mobilization in BAFCs. UTP (10 μM) was added at 50 s after the beginning of fluorescence determination. Typical tracings in the 3 experiments are shown. B: Effects of U73122 on UTP-induced $[Ca^{2+}]_i$ mobilization in BAFCs. BAFCs were preincubated with U73122 and demethylsulfoxide for 10 min at 30°C. UTP (10 μM) was added at 50 s after the beginning of fluorescence determination. Typical tracings in 3 experiments are shown.

Effect of ML-9 on CPA- and TG-induced $[Ca^{2+}]_i$ mobilization

CPA (100 μM), an inhibitor of Ca^{2+}-ATPase of ER (22), was added on fura 2-loaded BAFCs on a coverslip in the presence of extracellular Ca^{2+} (1.2 mM). CPA increased $[Ca^{2+}]_i$ gradually in BAFCs, and the increase in

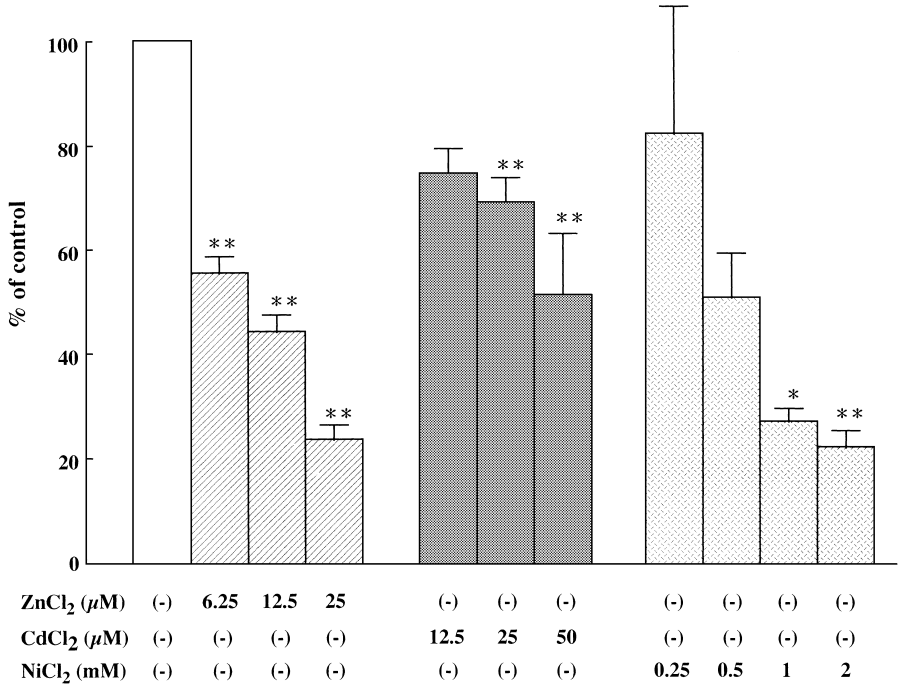

Fig. 2. Effects of Zn^{2+}, Cd^{2+}, and Ni^{2+} on UTP-induced $[Ca^{2+}]_i$ mobilization in BAFCs. Ratio from basal line at 200 s after the beginning of fluorescence determination was 100% in the absence of each cation. Each value represents the mean ± S.D. from 3 experiments. Statistically different from the control value (*P<0.05, **P<0.01).

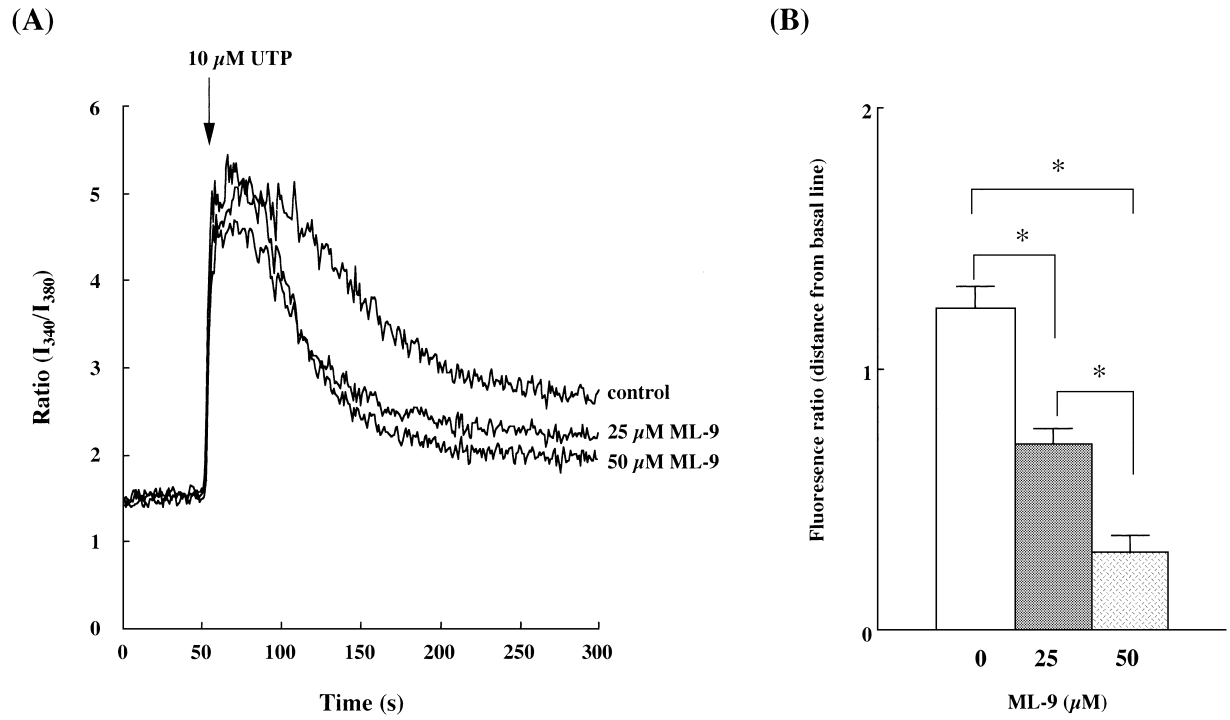

Fig. 3. Effect of ML-9 on UTP-induced $[Ca^{2+}]_i$ mobilization in BAFCs. UTP (10 μM) was added at 50 s after the beginning of fluorescence determination in the presence of extracellular Ca^{2+} (1.2 mM). Cells were pretreated with ML-9 for 10 min before the addition of UTP. A: Typical tracings in 3 experiments are shown. B: The ratio of the fluorescence intensity at 250 s after the beginning of fluorescence determinations. Statistically different from the control value (*P<0.05). Each value represents the mean ± S.D.

$[Ca^{2+}]_i$ by CPA was sustained (Fig. 4A). The preincubation with ML-9 (25 and 50 μM) for 10 min attenuated the sustained phase by CPA in a concentration-dependent manner (Fig. 4A). The addition of another Ca^{2+}-ATPase inhibitor, TG (2 μM) (23), in the absence of extracellular Ca^{2+} produced a transient increase in $[Ca^{2+}]_i$ due to release of Ca^{2+} from ER, an intracellular Ca^{2+} store; and the addition of Ca^{2+} (1.2 mM) in the incubation medium evoked a rapid and sustained increase in $[Ca^{2+}]_i$ (Fig. 4B). The increase in $[Ca^{2+}]_i$ evoked by the addition of extracellular Ca^{2+} on the TG-treated cells was also inhibited by the ML-9 pretreatment in a concentration-dependent manner (Fig. 4B).

Effects of W-7 and E6 berbamine on UTP-induced $[Ca^{2+}]_i$ mobilization

W-7, a calmodulin inhibitor (24), attenuated the Ca^{2+} entry from an extracellular pool evoked by 10 μM UTP in a concentration-dependent manner (25 – 100 μM) (Fig. 5A). The inhibitory effect of W-7 (50 and 100 μM) on the second phase was statistically different from the control value (P<0.05). However, 100 μM W-5, an inactive W-7 derivative (24), did not affect the effect of UTP (Fig. 5A). E6 berbamine (40 μM), another calmodulin inhibitor (25), also inhibited the second phase in UTP-induced $[Ca^{2+}]_i$ mobilization in BAFCs (Fig. 5B). The effect of the agent was statistically different from control value (P<0.05). Because the involvement of Ca^{2+}/CaM kinase II on SOCs activation was suggested (26, 27), we examined the effect of KN-62, a specific inhibitor of Ca^{2+}/CaM kinase II (28), on UTP-induced $[Ca^{2+}]_i$ mobilization. However, 10 μM KN-62 did not inhibit the effect of UTP (data not shown).

Effect of ML-9 on the actin-network

F-actin in the control BAFCs were stained with rhodamine-phalloidin. Figure 6A shows the fluorescence pattern of these cells exhibiting the morphology common to fibroblasts and other cell types. Stress fiber composed of F-actin distributed parallel or convergent to each other across the cell, and polygonal array of F-actin around the cell edge were stained. Some punctate fluorescence was found in the cytoplasm. In some other cells, bundles of F-actin arranged circumferentially around the perinuclear accumulation of cytoplasmic granules. BAFCs were treated with 50 – 100 μM ML-9 for 10 – 30 min and stained with rhodamine-phalloidin. The bulk of the stress fibers and the circumferential

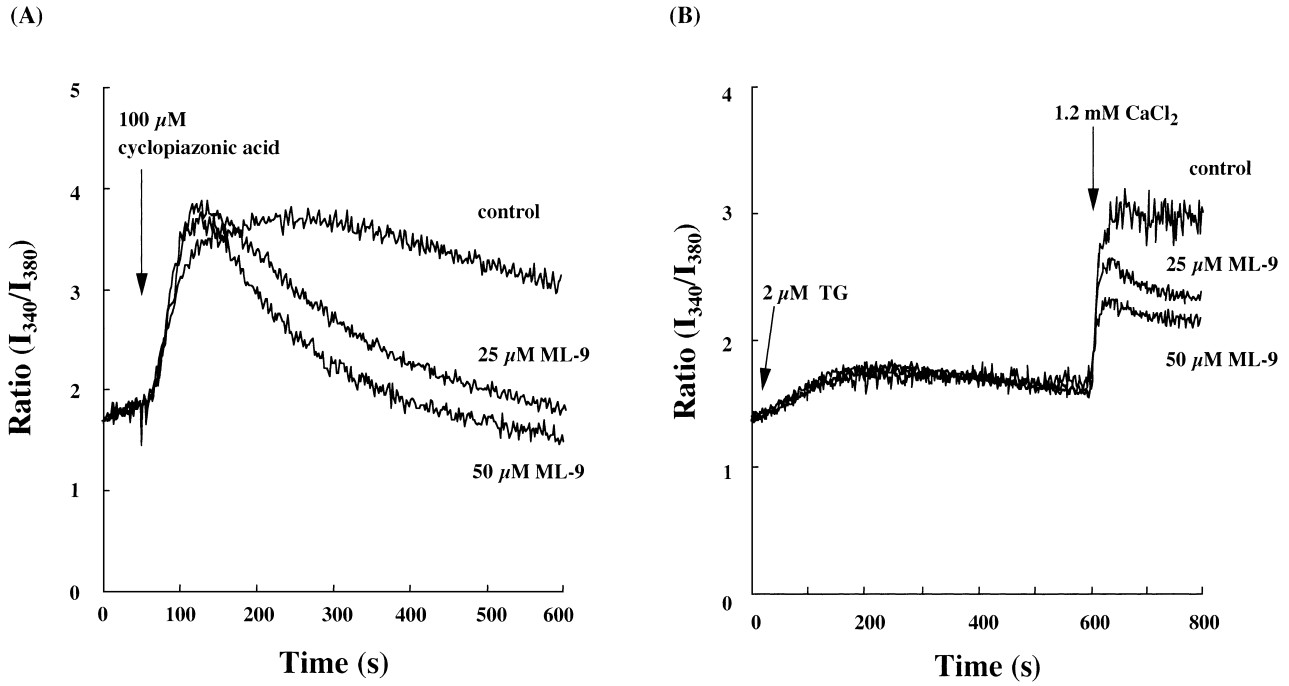

Fig. 4. Effect of ML-9 on CPA- and TG-induced $[Ca^{2+}]_i$ mobilization in BAFCs. A: Effect of ML-9 on CPA-induced $[Ca^{2+}]_i$ mobilization in BAFCs. Cells were pretreated with ML-9 for 10 min before the addition of CPA. CPA (100 μM) was added at 50 s after the beginning of fluorescence determination in the presence of extracellular Ca^{2+} (1.2 mM). Typical tracings in 3 experiments are shown. B: Effect of ML-9 on TG-induced $[Ca^{2+}]_i$ mobilization in BAFCs. Cells were pretreated with ML-9 for 10 min before the addition of TG. TG (2 μM) was added just after the beginning of fluorescence determination in the absence of extracellular Ca^{2+}. The increase in the intracellular Ca^{2+} was detected by the addition of 1.2 mM Ca^{2+}. Typical tracings in the 3 (A) and 2 (B) experiments are shown.

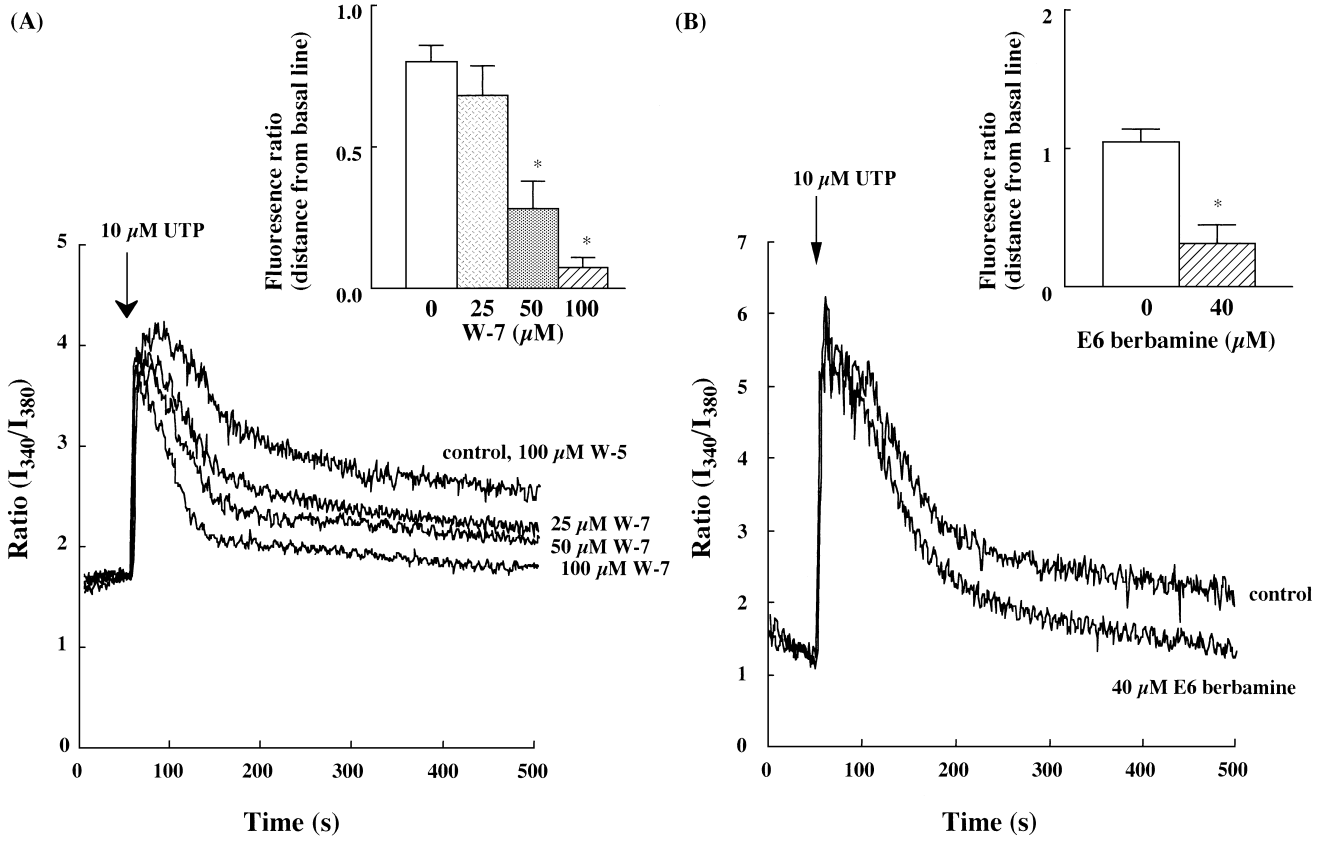

Fig. 5. Effects of calmodulin inhibitors on UTP-induced $[Ca^{2+}]_i$ mobilization in BAFCs. A: Effect of W-7 on UTP-induced $[Ca^{2+}]_i$ mobilization in BAFCs. Cells were pretreated with W-7 for 10 min before the addition of 10 μM UTP in the presence of extracellular Ca^{2+} (1.2 mM). Typical tracings in the 4 experiments are shown. The inset is the ratio of the fluorescence intensity at 400 s after the beginning of fluorescence determination. Statistically different from the control value (*P<0.05). Each value represents the mean ± S.D. B: Effect of E6 berbamine on UTP-induced $[Ca^{2+}]_i$ mobilization in BAFCs. Cells were pretreated with E6 berbamine for 20 min before the addition of 10 μM UTP in the presence of extracellular Ca^{2+} (1.2 mM). Typical tracings in the 6 experiments are shown. The inset is the ratio of the fluorescence intensity at 400 s after the beginning of fluorescence determination. Statistically different from the control value (*P<0.05). Each value represents the mean ± S.D.

F-actin bundles were missing and polygonal arrays of F-actin also decreased, although some fine F-actin remained. On the contrary, punctuate fluorescence numerously increased in the treated cells (Fig. 6: B, C, D) and tail-shaped fluorescence, which was never found in the control cells, appeared (Fig. 6E), suggesting that ML-9 had disrupted stress fibers and other F-actin bundles. The effects of ML-9 on F-actin were increased with its concentration and the duration time of the treatment.

Effects of W-7 and E6 berbamine on the actin-network

BAFCs treated with 100 μM W-7 for 10 min and 40 μM E6 berbamine for 20 min were stained with rhodamine-phalloidin. The bulk of stress fibers, circumferential and polygonal arrays of F-actin, in both treated cells became less in comparison with the control cells, although the amount of punctate fluorescence increased, as in the case of ML-9 treatment (Fig. 7). These results suggest that W-7 and E6 berbamine had disrupted the actin-network.

Effect of cytochalasin D on UTP-induced $[Ca^{2+}]_i$ mobilization and the actin-network

UTP-induced $[Ca^{2+}]_i$ mobilization in BAFCs was inhibited by the pretreatment of 25 μM cytochalasin D (Fig. 8A). The reagent attenuated the first phase slightly. Cytochalasin D also disturbed the actin-network (Fig. 8B).

Discussion

In BAFCs, UTP augments Ca^{2+} entry from an extracellular pool in a VOC inhibitor-insensitive manner subsequent to stimulating Ca^{2+} release from intracellular stores. Although specific inhibitors on SOCs are still unavailable, the UTP-induced Ca^{2+} entry is inhibited by

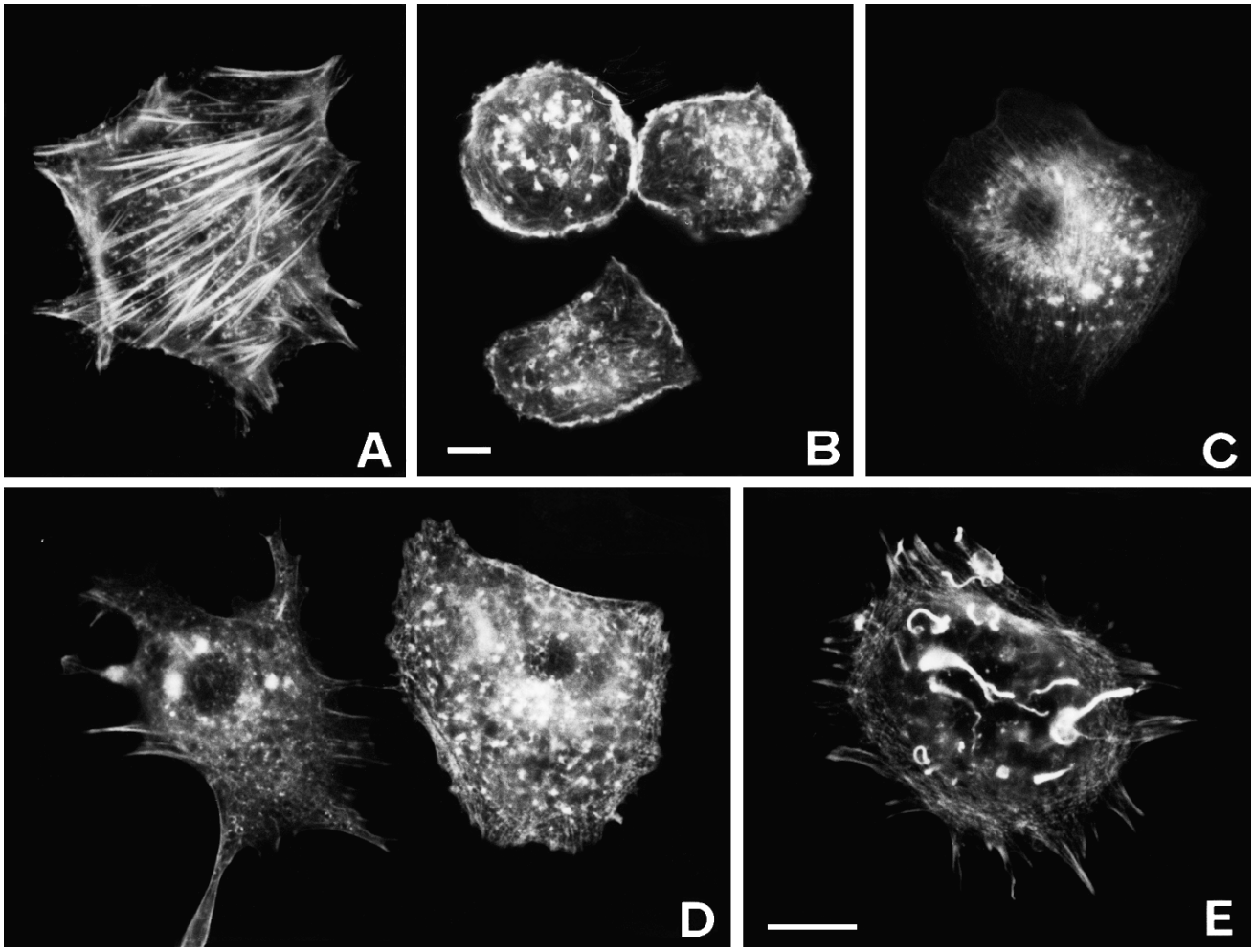

Fig. 6. Effect of ML-9 on F-actin in BAFCs. A: Typical fluorescent images of stress fibers, polygonal arrays and punctate structure of actin are visible in the cell. B – E: BAFC treated with 50 μM ML-9 for 10 min (B, C), 20 min (D), or 30 min (E). Stress fibers and other F-actin were disrupted. On the contrary, the amount of punctate fluorescence increased with the duration time of the treatment (B – D) and tail-shaped fluorescence appeared (E). A, C – E: ×600, B: ×375; Bar: 20 μM.

I_{CRAC} inhibitors, Zn^{2+}, Cd^{2+}, and Ni^{2+}, in the similar potency order, $Zn^{2+} > Cd^{2+} \gg Ni^{2+}$, as previously reported (20).

It is proposed that SOCs are triggered by Ca^{2+} depletion from ER, one of the intracellular Ca^{2+} stores (29). The depletion of luminal Ca^{2+} in ER is achieved by $InsP_3$ and the inhibitors of Ca^{2+}-ATPase in ER. Nishi (9) reported that UTP enhanced $InsP_3$ production via $P2Y_2$ receptors in BAFCs. In our experimental condition, a phospholipase C inhibitor, U73122, inhibited UTP-induced Ca^{2+} entry accompanied by the decrease of Ca^{2+} release from ER. Therefore, UTP should increase $[Ca^{2+}]_i$ due to SOCs activation in BAFCs.

Precise components of SOCs have not yet been clarified. However, the possible involvement of some members of the TRP family in SOCs has been recently reported as candidates for the components of SOCs (30). The member of the TRP family remain to be identified, and the involvement of the TRP in UTP-induced $[Ca^{2+}]_i$ mobilization in BAFCs must be elucidated.

Although there are many reports with respect to the mechanisms of SOCs activation in several kinds of cells, no consensus for how such a mechanism takes place has been reached (1). However, there are two main routes to explain SOCs activation, one is the production of a diffusible factor (31) and other is the conformational coupling mechanism (32). The latter hypothesis was derived from the observation of Rossier et al. (33). They reported that calcium-storing $InsP_3$-sensitive organelles were linked to plasma membrane through F-actin in rat liver cells. Their observation suggests that the interaction between ER and F-actin is one of the important factors in the conformational coupling model. The close linkage between ER and F-actin were also suggested in

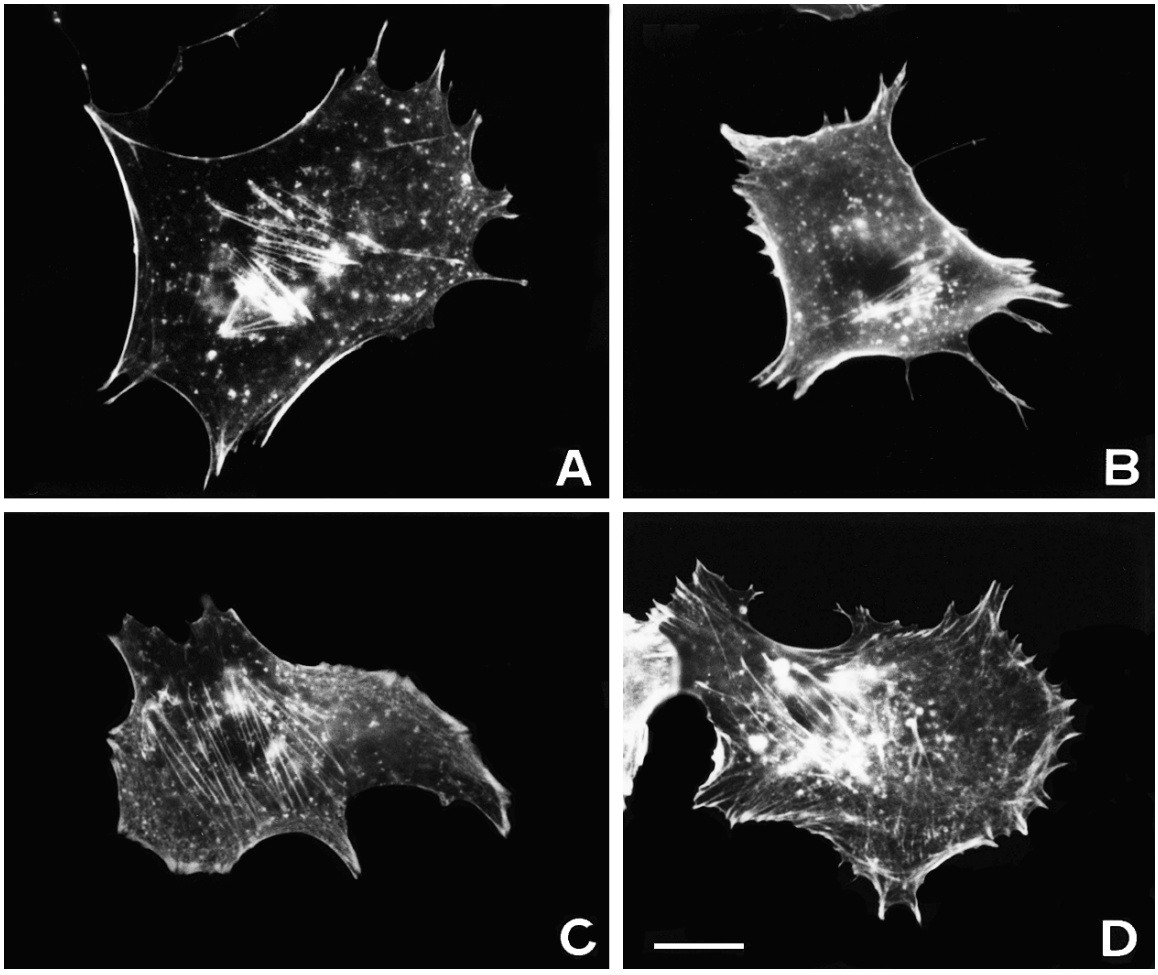

Fig. 7. Effects of W-7 and E6 berbamine on F-actin in BAFCs. A, B: BAFCs were treated with 100 μM W-7 for 10 min. C, D: BAFCs were treated with 40 μM E6 berbamine for 20 min. The bulk of F-actin in both treated cells became less in comparison with that in the control cells. A – D: ×600; Bar: 20 μM.

bovine adrenal cortex (34), Krebs II ascites tumor cells (35), and honeybee photoreceptor cells (36, 37).

In the present study, the inhibition of calcium/calmodulin-dependent MLCK by ML-9, a MLCK inhibitor, and calmodulin inhibitors attenuated UTP-induced Ca^{2+} entry and depolymerized F-actin in BAFC. These results suggest that MLCK might play an important role in retaining the integrity of the actin network, and destabilization of the intact F-actin structure could disturb the interaction between ER and plasma membrane, resulting in SOCs inhibition. Another possibility is that phosphorylated myosin might move ER toward the plasma membrane along the stationary F-actin in BAFCs as Kachar and Reese (38) observed using electron microscopy in characean ALGOL cells. Whether either or both, the intact F-actin is obligatory for the regulation of SOCs. However, as a high concentration of ML-9 might inhibit protein kinase C and protein kinase A, it does not deny the possible involvement of protein kinase C (11) and protein kinase A (39) in SOCs activation in BAFCs.

Holda and Blatter (40) showed that cytochalasin D treatment inhibited TG-induced Ca^{2+} entry, but did not affect the release of Ca^{2+} from intracellular stores through $InsP_3$ production by ATP in CPAE vascular endothelial cells, whose cell line was originally derived from calf pulmonary artery endothelium, concomitant with F-actin disruption. Furthermore, we observed that cytochalasin D inhibited UTP-induced $[Ca^{2+}]_i$ mobilization and depolymerizes the F-actin network in BAFC. However, cytochalasin D slightly inhibited the first phase. The result suggests that cytochalasin D might affect $InsP_3$ production by UTP in BAFC. It had been reported that cytochalasin D inhibited phospholipase C by disturbing the actin-network in human mammary epithelial cells (41) and the pancreatic aciner tumor cell line

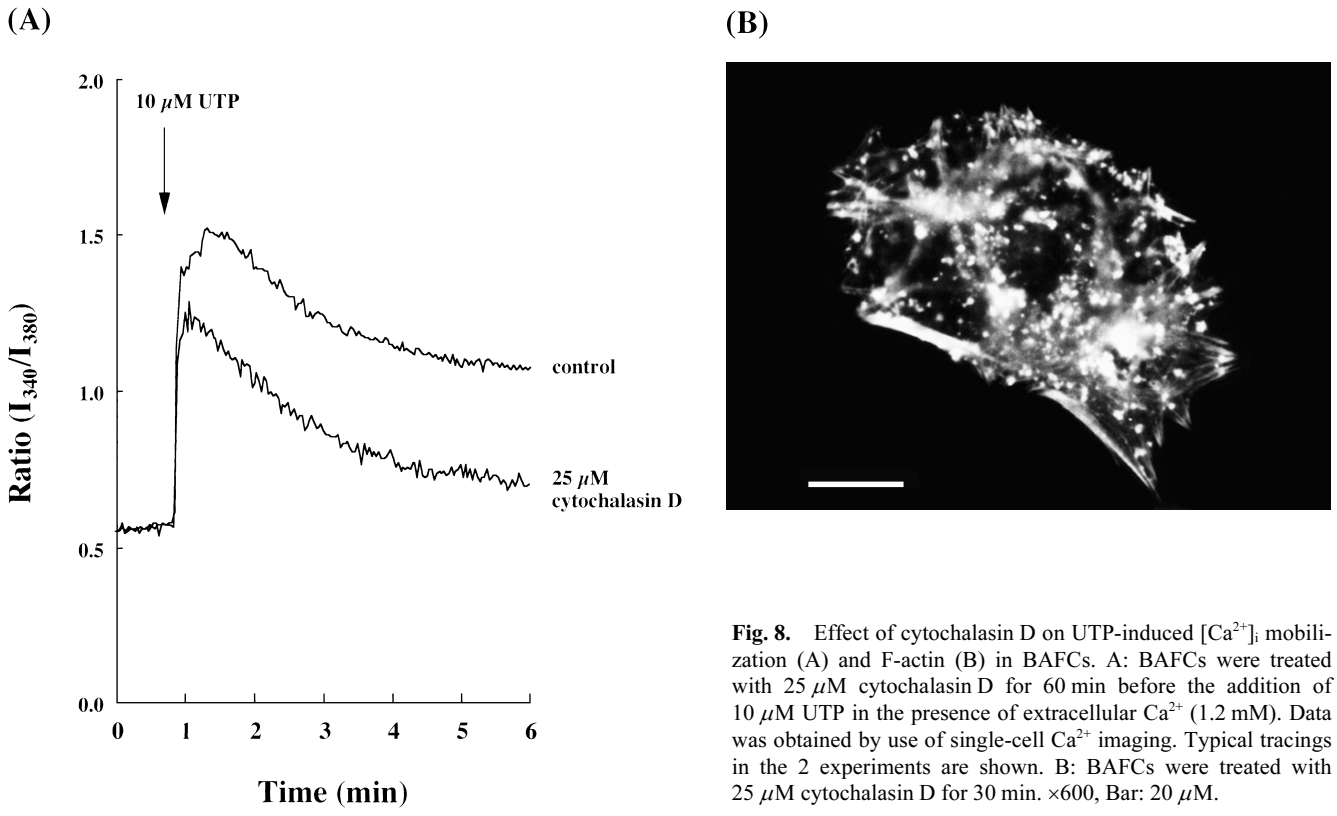

Fig. 8. Effect of cytochalasin D on UTP-induced $[Ca^{2+}]_i$ mobilization (A) and F-actin (B) in BAFCs. A: BAFCs were treated with 25 μM cytochalasin D for 60 min before the addition of 10 μM UTP in the presence of extracellular Ca^{2+} (1.2 mM). Data was obtained by use of single-cell Ca^{2+} imaging. Typical tracings in the 2 experiments are shown. B: BAFCs were treated with 25 μM cytochalasin D for 30 min. ×600, Bar: 20 μM.

AR4-2J (42). In BAFCs, ML-9 did not attenuate the first phase in UTP-induced $[Ca^{2+}]_i$ mobilization in spite of the disturbance of the actin-network. Therefore, in our experimental condition, the possibility that cytochalasin D may have some direct inhibitory effect on $InsP_3$ producing cascade can not be denied. Watanabe et al. (14) and Takahashi et al. (15) reported the inhibitory effect of ML-9 on TG- and agonist-induced Ca^{2+} influx in porcine aortic endothelial cells. Although the morphological studies were not reported in those articles, they speculated the involvement of the cytoskeleton in Ca^{2+} entry induced by Ca^{2+} store depletion. In rat hepatocyte, it has been reported that $InsP_3$ receptors localized sub-regions of ER interact with the plasma membrane through F-actin (43, 44). Rosado and Sage (45) also showed the involvement of intact actin cytoskeleton in SOCs activation in platelets. They concluded that ER transport toward the plasma membrane was an important process in SOCs activation (46). These reports and our results strongly suggest that the interaction between ER and plasma membrane mediated by F-actin plays a pivotal role in SOCs regulation. However, Ribeiro et al. (47), by contrast, reported that depolymeryzation of F-actin by cytochalasin D inhibited ATP- and platelet derived growth factor-elicited Ca^{2+} influx but not TG-induced Ca^{2+} influx in the NIH3T3 cell line; and Bakowski et al. (48) showed that both the stabilization and disruption of F-actin did not inhibit IP_3-induced I_{CRAC} activation in RBL-1 rat basophilic cell line. They proposed that an intact actin cytoskeleton was not necessary for SOCs activation. Also, Patterson et al. (49) showed that disruption of F-actin with cytochalasin D did not inhibit SOCs in DDT1MF-2 smooth muscle cells. On the contrary, jasplakinolide, the marine sponge toxin, which induces polymerization and stabilization of F-actin (50) caused a dense accumulation of F-actin in the periphery and inhibited Ca^{2+} entry by TG. They conclude that the cortical dense F-actin layer displaced ER some distance away from the plasma membrane to inhibit SOCs. The reason for these discrepancies is not clear, but there might be qualitative and quantitative differences on F-actin structure and/or the localization of ER between the cell types or primary cultured cells and the passed cell lines (51). To certify the close relation between the $[Ca^{2+}]_i$ mobilization and the dynamic change of the actin-network in SOCs activation in BAFCs, the real-time determination of both phenomena in a single cell remains to be studied in BAFC.

Although several mechanisms might be involved in the regulation of SOCs in different cell types (52), our results strongly suggest that, in BAFCs, actin network

integrity seems to be important for the activation of SOCs. Thus it would be obligatory to maintain the spatiotemporal integrity among plasma membrane, actin-network, and ER to enable UTP-induced SOCs activation in BAFCs.

Acknowledgments

This study was supported in part by the Japan Human Sciences Foundation and the Science Research Promotion Fund from the Promotion and Mutual Aid Corporation for Private Schools of Japan.

References

1 Barritt GJ: Receptor-activated Ca^{2+} inflow in animal cells: a variety of pathways tailored to meet different intracellular Ca^{2+} signaling requirements. Biochem J **337**, 153 – 169 (1999)
2 Putney JW Jr and Bird GS: The inositol phosphate-calcium signaling system in nonexcitable cells. Endocr Rev **14**, 610 – 631 (1993)
3 Parekh AB and Penner R: Store depletion and calcium influx. Physiol Rev **77**, 901 – 930 (1997)
4 Dubyak GR and El-Moatassim C: Signal transduction via P2-purinergic receptors for extracellular ATP and other nucleotides. Am J Physiol **265**, C577 – C606 (1993)
5 Burnstock G: The past, present and future of purine nucleotides as signalling molecules. Neuropharmacology **36**, 1127 – 1139 (1997)
6 Kawamura M, Matsui T, Niitsu A, Kondo T, Ohno Y and Nakamichi N: Extracellular ATP stimulates steroidogenesis in bovine adrenocortical fasciculata cells via P2 purinoceptors. Jpn J Pharmacol **56**, 543 – 545 (1991)
7 Kawamura M, Niitsu A, Nishi H and Masaki E: Extracellular ATP potenciates steroidogenic effect of adrenocorticotropic hormone in bovine adrenocortical fasciculata cells. Jpn J Pharmacol **85**, 376 – 381 (2001)
8 Hoey ED, Nicol M, Williams SC and Walker SW: Primary cultures of bovine inner zone adrenocortical cells secrete cortisol in response to adenosine triphosphate, adenosine diphosphate, and uridine triphosphate via a nucleotide receptor which may be coupled to two signal generation systems. Endocrinology **134**, 1553 – 1560 (1994)
9 Nishi H: Two different P2Y receptors linked to steroidogenesis in bovine adrenocortical cells. Jpn J Pharmacol **81**, 194 – 199 (1999)
10 Ralevic V and Burnstock G: Receptors for purines and pyrimidines. Pharmacol Rev **50**, 413 – 492 (1998)
11 Kondo I: Protein kinase C potentiates capacitative Ca^{2+} entry that links to steroidogenesis in bovine adrenocortical cells. Jpn J Pharmacol **82**, 210 – 217 (2000)
12 Janmey PA: The cytoskeleton and cell signalling: Component localization and mechanical coupling. Physiol Rev **78**, 763 – 781 (1998)
13 Kim YC, Kim SJ, Kang TM, Suh SH, So I and Kim KW: Effects of myosin light chain kinase inhibitors on carbachol-activated nonselective cationic current in guinea-pig gastric myocytes. Pflugers Arch **434**, 346 – 353 (1997)
14 Watanabe H, Takahashi R, Zhang XX, Kakizawa H, Hayashi H and Ohno R: Inhibition of agonist-induced entry in endothelial cells by myosin light-chain kinase inhibitor. Biochem Biophys Res Commun **225**, 777 – 784 (1996)
15 Takahashi R, Watanabe H, Zhang XX, Kakizawa H, Hayashi H and Ohno R: Roles of inhibitors of myosin light chain kinase and tyrosine kinase on cation influx in agonist-stimulated endothelial cells. Biochem Biophys Res Commun **235**, 657 – 662 (1997)
16 Matsui T: Biphasic rise caused by extracellular ATP in intracellular calcium concentration in bovine adrenocortical fasciculata cells. Biochem Biophys Res Commun **178**, 1266 – 1272 (1991)
17 Ebisawa T, Kondo I, Masaki E, Hori S and Kawamura M: Capacitative calcium entry is involved in steroidogenesis in bovine adrenocortical fasciculata cells. J Endocrinol **167**, 473 – 478 (2000)
18 Tang S, Morgan KG, Parker C and Ware JA: Requirement for protein kinase C for cell cycle progression and formation of action stress fibers and filopodia in vascular endothelial cells. J Biol Chem **272**, 28704 – 28711 (1997)
19 Bleasdale JE, Thakur NR, Gremban RS, Bundy GL, Fitzpatrick FA, Smith RJ and Bunting S: Selective inhibition of receptor-coupled phospholipase C-dependent processes in human platelets and polymorphonuclear neutrophils. J Pharmacol Exp Ther **255**, 756 – 768 (1990)
20 Hoth M and Penner R: Calcium release-activated calcium current in rat mast cells. J Physiol (Lond) **465**, 359 – 386 (1993)
21 Saitoh M, Ishikawa T, Matsushima S, Naka M and Hidaka H: Selective inhibition of catalytic activity of smooth muscle myosin light chain kinase. J Biol Chem **262**, 7796 – 7801 (1987)
22 Seidler NW, Jona I, Vegh M and Martonosi A: Cyclopiazonic acid is a specific inhibitor of the Ca^{2+}-ATPase of sarcoplasmic reticulum. J Biol Chem **264**, 17816 – 17823 (1989)
23 Thastrup O, Dawson AP, Scharff O, Foder B, Cullen PJ, Drobak BK, Bjerrum PJ, Christensen SB and Hanley MR: Thapsigargin, a novel molecular probe for studying intracellular calcium release and storage. Agents Actions **27**, 17 – 23 (1989)
24 Hidaka H, Sadaki Y, Tanaka T, Endo T, Ohno S, Fujii Y and Nagata T: *N*-(6-Aminohexyl)-5-chloro-1-naphthalenesulfonamide, a calmodulin antagonist, inhibits cell proliferation. Proc Natl Acad Sci USA **78**, 4354 – 4357 (1981)
25 Hu ZY, Gong YS and Huang WL: Interaction of berbamine compound E6 and calmodulin-dependent myosin light chain kinase. Biochem Pharmacol **44**, 1543 – 1547 (1992)
26 Tornguist K and Ekokoshi E: Inhibition of agonist-mediated calcium entry by calmodulin antagonists and the Ca^{2+}/calmodulin kinase II inhibitor KN-62. Studies with thyroid FRTL-5 cells. J Endocrinol **148**, 131 – 138 (1996)
27 Puhl HL, Raman PS, Williams CL and Aronstam RS: Inhibition of M3 muscarinic acetylcholine receptor-mediated Ca^{2+} influx and intracellular mobilization in neuroblastoma cells by the Ca^{2+}/calmodulin-dependent protein kinase inhibitor, 1-[*N*,*O*-bis(5-isoquinolinesulfonyl)-*N*-methyl-L-tyrosyl]-4-phenylpiperazine (KN-62). Biochem Pharmacol **53**, 1107 – 1114 (1997)
28 Tokumitsu H, Chijiwa T, Hagiwara M, Mizutani A, Terasawa M and Hidaka H: KN-62, 1-[*N*,*O*-bis(5-isoquinolinesulfonyl)-*N*-methyl-L-tyrosyl]-4-phenylpiperazine, a specific inhibitor of Ca^{2+}/calmodulin-dependent protein kinase II. J Biol Chem **265**, 4315 – 4320 (1990)

29 Putney JW Jr: A model for receptor-regulated calcium entry. Cell Calcium **7**, 1 – 12 (1986)

30 Zitt C, Halaszovich CR and Luckhoff A: The TRP family of cation channels: probing and advancing the concepts on receptor-activated calcium entry. Prog Neurobiol **66**, 243 – 264 (2002)

31 Randriamampita C and Tsien RY: Emptying of intracellular Ca^{2+} stores releases a novel small messenger that stimulates Ca^{2+} influx. Nature **364**, 809 – 814 (1995)

32 Berridge MJ: Capacitative calcium entry. Biochem J **312**, 1 – 11 (1995)

33 Rossier MF, Bird GSJ and Putney JW Jr: Subcellular distribution of the calcium-storing inositol 1,4,5-trisphosphate-sensitive organelle in rat liver. Biochem J **274**, 643 – 650 (1991)

34 Guillemette G, Favreau I, Boulay G and Potier M: Solubilization and partial characterization of inositol 1,4,5-trisphosphate receptor of bovine adrenal cortex reveal similarities with receptor of rat cerebellum. Mol Pharmacol **38**, 841 – 847 (1990)

35 Fjose A and Pryme IF: Altered distribution profiles of endoplasmic reticulum subfractions after incubation of Krebs II ascites cells with different concentrations of cytochalasin B. Cell Biochem Funct **2**, 38 – 42 (1984)

36 Baumann O: Structural interactions of actin filaments and endoplasmic reticulum in honeybee photoreceptor cells. Cell Tissue Res **268**, 71 – 79 (1992)

37 Baumann O and Lautenschlager B: The role of actin filaments in the organization of the endoplasmic reticulum in honeybee photoreceptor cells. Cell Tissue Res **278**, 419 – 432 (1994)

38 Kachar B and Reese TS: The mechanism of cytoplasmic streaming in characean algal cells: sliding of endoplasmic reticulum along actin filaments. J Cell Biol **106**, 1545 – 1552 (1988)

39 de la Rosa LA, Vlarino N, Vieytes MR and Botana LM: Modulation of thapsigargin-induced calcium mobilization by cyclic AMP-elevating agents in human lymphocytes is insensitive to the action of the protein kinase A inhibitor H-89. Cell Signal **13**, 441 – 449 (2001)

40 Holda JR and Blatter LA: Capacitative calcium entry is inhibited in vascular endothelial cells by disruption of cytoskeletal microfilaments. FEBS Lett **403**, 191 – 196 (1997)

41 Suzuki K and Takahashi K: Actin filament assembly and actin-myosin contractility are necessary for anchorage- and EGF-dependent activation of phospholipase Cγ. J Cell Physiol **189**, 64 – 71 (2001)

42 Bozem M, Kuhlmann S, Blum R, Feick P and Schulz I: Hormone-stimulated calcium release is inhibited by cytoskeleton-disrupting toxins in AR4-2J cells. Cell Calcium **28**, 73 – 82 (2000)

43 Lievremont J-P, Hill A-M, Hilly and M Mauger J-P: The inositol 1,4,5-trisphosphate receptor is localized on spicialized subregions of the endoplasmic reticulum in rat liver. Biochem J **300**, 419 – 427 (1994)

44 Gregory RB, Wilcox RA, Berven LA, van Straten NCR, van der Marel GA, van Boom JH and Barrit GJ: Evidence for the involvement of a small subregion of the endoplasmic reticulum in the inositol trisphosphate receptor-induced activation of Ca^{2+} inflow in rat hepatocytes. Biochem J **341**, 401 – 408 (1999)

45 Rosado JA and Sage SO: A role for the actin cytoskeleton in the initiation and maintenance of store-mediated calcium entry in human platelets. Trends Cardiovasc Med **10**, 327 – 332 (2000)

46 Rosado JA, Jenner S and Sage SO: A role for the actin cytoskeleton in the initiation and maintenance of store-mediated calcium entry in human platelets. Evidence for conformational coupling. J Biol Chem **275**, 7527 – 7533 (2000)

47 Ribeiro CMP, Reece J and Putney JW Jr: Role of the cytoskeleton in calcium signaling in NIH 3T3 cells. An intact cytoskeleton is required for agonist-induced $[Ca^{2+}]_i$ signaling but not for capacitative calcium entry. J Biol Chem **272**, 26555 – 26561 (1997)

48 Bakowski D, Glitsch MD and Parekh AB: An examination of the secretion-like coupling model for the activation of the Ca^{2+} release-activated Ca^{2+} current I_{CRAC} in RBL-1 cells. J Physiol (Lond) **532**, 55 – 71 (2001)

49 Patterson RL, van Rossum DB and Gill DL: Store-operated Ca^{2+} entry: Evidence for a secretion-like coupling model. Cell **98**, 487 – 499 (1999)

50 Bubb MR, Senderowicz AMJ, Sausville EA, Duncan KLK and Korn ED: Jasplakinolide, a cytotoxic natural product, induces actin polymerization and competitively inhibits the binding of phalloidin to F-actin. J Biol Chem **269**, 14869 – 14871 (1994)

51 Samain E, Bouillier H, Perret C, Safer M and Dagher G: ANG II-induced increase in smooth muscle cells from SHR is regulated by actin and microtuble networks. Am J Physiol **277**, H834 – H841 (1999)

52 Putney JW Jr, Broad LM, Braun FJ, Lievremont JP and Bird GS: Mechanisms of capacitative calcium entry. J Cell Sci **114**, 2223 – 2229 (2001)